JOURNAL OF NANO- AND ELECTRONIC PHYSICS
Vol. 5 No 2, 02015(5pp) (2013)

ЖУРНАЛ НАНО- ТА ЕЛЕКТРОННОЇ ФІЗИКИ
Том 5 № 2, 02015(5cc) (2013)

Fabrication and Characterization of Al/*p*-CuInAlSe$_2$ Thin Film Schottky Diodes

Usha Parihar[1,*], N. Padha[1], C.J. Panchal[2]

[1] *Department of Physics& Electronics, University of Jammu, Jammu, 180006 J&K, India*
[2]*M.S. University of Baroda, Faculty of Technology and Engineering, 390 009 Vadodara, India*

(Received 15 February 2013; published online 04 May 2013)

Al/*p*-CuInAlSe$_2$ polycrystalline schottky diodes fabricated by flash evaporation method were undertaken for their electrical analysis at room temperature. Diode parameters of the undertaken diodes were then derived from the current-voltage (I-V) as well as capacitance-voltage (C-V) characteristics. It has been observed that the schottky barrier height deduced from the room temperature I-V is lower to that obtained from the C-V characteristics and is attributed to the fact that I-V analysis includes both the image force and dipole lowering effects and is also reduced by the tunneling and leakage currents. The slope variation of the frequency dependent C^{-2}-V characteristics for the Al/*p*-CuInAlSe$_2$ Schottky diode at varying frequency values from 50 kHz to 1 MHz suggests a large density of slow traps or interface states at the M-S junction. As emerging from the parameters values energy band diagram of Al and P-CuInAlSe$_2$ has been reconstructed.

Keywords: Polycrystalline, schottky diodes, Flash evaporation, Current-voltage (I-V), Capacitance-voltage (C-V) characteristics, Image force, Dipole lowering effects, Interface states, M-S junction template.

PACS numbers: 73.40.QV, 73.61.Ey, 85.30 Hi

1. INTRODUCTION

Cu(In, Al)Se$_2$ is a direct bandgap quaternary semiconductor in which the bandgap can be controlled from 1.0 eV (CIS) to 2.7 eV (CuAlSe$_2$) by substitution of Al to In [1]. This makes it a potential candidate for low cost solar cells. As on today two kinds of photovoltaic devices exists differing from each other through production method. One of these is in the form of schottky junction whereas another one is in the form of *p*-*n* junction (homojunction or hetrojunction). The later can be made of the same semiconductor by different type doping, yielding relatively more complex structure compared to M-S one [2, 3].Further, M-S structures forms an important research tools in the characterization of new semiconductor materials and at the same time, the fabrication of these structures plays a vital role in constructing some useful devices in technology [4, 5]. The electrical properties of the schottky contacts depend on the density of interface states which play crucial role on determination of diode parameters such as schottky barrier height (φ_b) and ideality factor (η). Besides, the control of interface property is very promising for device performance, stability and reliability [5-7].

In view of this, we first time report the fabrication of Al/*p*-CuInAlSe$_2$ polycrystalline schottky diodes over flash evaporated CIAS thin films. Their current-voltage (I-V) as well as capacitance-voltage (C-V) characteristics has been measured at room temperature and various junction parameters were calculated.

2. EXPERIMENTAL

Polycrystalline CuIn$_{1-x}$Al$_x$Se$_2$ (CIAS) material with $x = 0.19$ was prepared by reacting all the constituent elements with appropriate proportion in weight in an evacuated quartz ampoule at1400 K at the rate of 3 K / min. The composition as well as structure of the material was established from EDAX and XRD analysis respectively. It was then used as a source material for depositing CuIn$_{0.81}$Al$_{0.19}$Se$_2$ (CIAS) thin films on organically cleaned sodalime glass substrates held at 473 K by flash evaporation technique. The rate of deposition was maintained at 0.2-0.3 nm/s and typical thickness of the film was 500 nm was obtained which was continuously monitored during the deposition using a quartz crystal thickness monitor DTM-101 (HindHiVac., India). The substrate temperature was measured using Chromel-Alumel Thermocouple kept in good thermal contact with the substrate. The deposited films were also thermally annealed at 573 K in a vacuum chamber at a base pressure of 10^{-2} mbar for 1 h. The films were found to be *p*-type as determined by Hall experiment. The Schottky diodes of the area 9×10^{-2}cm^2 were prepared by depo-siting Aluminum thin films over the deposited CIAS thin layer. The structure of CIAS based Schottky diode is shown in Fig. 1 where CIAS layer act as a *P*-type semiconductor and Aluminum(Al) forms a schottky contact while Silver (Ag) acts as a back ohmic contact. The thicknesses of silver and aluminum films were kept to be 150 nm and 250 nm respectively. The current-voltage (I-V) characteristics of Al/*p*-CuInAlSe$_2$ schottky diodes were measured at room temperature by using Probe Station and Keithley's Source Meter (Model 2400). The data of current-voltage measurements were recorded to a personal computer using GPIB data transfer card.

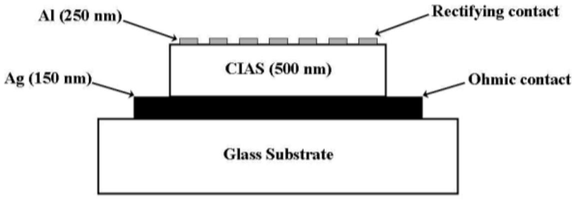

Fig. 1 – The cross-sectional schematic view of the structure of Al/*p*-CuInAlSe$_2$ Schottky diode

---

[*] pariusha@gmail.com

3. RESULTS AND DISCUSSION

3.1 Current-Voltage Characteristics

The forward and the reverse bias I-V a characteristics of Al/*p*-CuInAlSe$_2$ Schottky diode at room temperature are shown in Fig. 2. In the forward bias, the current increases exponentially with voltage, however, in reverse bias, the current measured within the given bias did not show any trend of breakdown. This could be due to the domination of edge leakage current and the presence of some thin oxide layer at the interface and also due to the generation of excess carriers in the depletion region at higher fields. The existence of SBH inhomogeneity offers a natural explanation for the soft reverse characteristics observed experimentally. For inhomogeneous MS contacts, the reverse current may be dominated by the current which flows through the low-SBH patches, which is controlled by the potential at the saddle point; hence, the reverse current increases with increasing reverse bias and does not saturate [8].

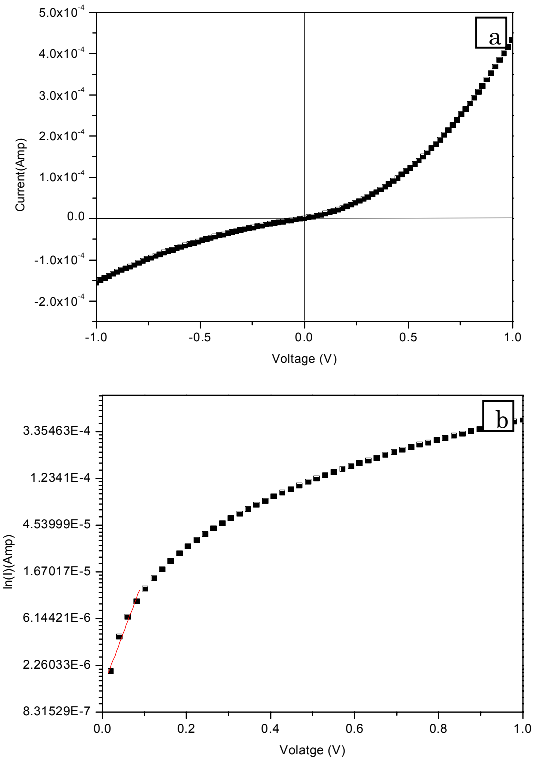

Fig. 2 – I-V characteristics of Al/*p*-CuInAlSe$_2$ Schottky diode (a), forward ln(I) vsV characteristics of Al/*p*-CuInAlSe$_2$ Schottky diode (b)

Also, the forward and the reverse bias I-V a characteristic of Al/*p*-CuInAlSe$_2$ schottky diode depicted a rectifying behaviour. Therefore, it can be assumed that the device behaves as a Schottky diode and the thermionic emission theory can be used to obtain electrical parameters of the device. Also, according to the thermionic emission theory net current can be determined through the relation [21]

$$I = I_s \left\{ \exp\left(\frac{q\left(V - IR_s\right)}{\eta KT} \right) - 1 \right\} \tag{1}$$

where I_s, the saturation current and J_s, the saturation current density, defined as:

$$J_s = \frac{I_s}{A} = A^{**}T^2 \exp\left(-\frac{q\varphi_{bo}}{kT} \right) \tag{2}$$

The quantities A is the diode area ($= 9 \times 10^{-2}$cm^2), A^{**} effective Richardson constant for *p*-type CuInSe$_2$, (30 A/cm^2) [18], T is the measurement temperature in Kelvin (303 K), k is Boltzmann's constant (1.38×10^{23} J/K), q is the electron charge (1.6×10^{-19} C), V is the forward applied voltage, φ_{bo} is the zero bias barrier height and R_s is the series resistance. The ideality factor η is a measure of conformity of the diode to pure thermionic emission and η is equal to 1 for pure thermionic emission [9]. For values of $V > 3kT/q$, the ideality factor using Eq. (1) can be expressed as

$$n = \frac{q}{kT}\left(\frac{dV}{d\ln(I)} \right) \tag{3}$$

The barrier height and ideality factor of Al/*p*-CuInAlSe$_2$ schottky diodes were found as 0.59 eV and 1.59 respectively, as determined from the intercept and slope of the forward-bias ln(I)-V plot by the help of Eqs. (2) and (3). The ideality factor greater than unity refers the deviation from an ideal diode, the deviation can be attributed the formation of thin interfacial layer and/or surface effects like, the surface charge and image force effects at Al/*p*-CuInAlSe$_2$ interface[10]. As can be seen in Fig. 1, the semi logarithmic I-V curves are nonlinear in nature. The results demonstrate that the nonlinearity in the current-voltage characteristics arises due to series resistance in a subtle way when a number of non-interacting parallel diodes with a Gaussian distribution of barrier heights act simultaneously. Consequently, the linearity of the ln(I)-V plot was found short and therefore according to S. Chand et al. that as the linear region of the forward ln(I)-V plots is reduced, the accuracy of the determination of φ_{bo} and η becomes poorer. Hence, same was not considered for extraction of barrier parameters (viz., φ_{bo} and η).

Therefore, to determine the barrier height and the series resistance an alternate approach developed by Norde [12] was used. This approach has been modified as [13]

$$F(V) = \frac{V}{\gamma} - \frac{kT}{q}\left(\frac{I(V)}{AA^{**}T^2} \right) \tag{4}$$

where γ is a the first integer greater than η and I(V) is the current obtained from the I-V curve. Here, γ has been taken as 2 and the barrier height of device can be obtained by using

$$\varphi_b = F(V_o) + \frac{V_o}{\gamma} - \frac{kT}{q} \tag{5}$$

where $F(V_0)$ is the minimum $F(V)$ value of F versus V graph and V_0 is the corresponding voltage. Fig. 3 shows the $F(V)$-V graph of the Al/*p*-CuInAlSe$_2$ Schottky diode. The series resistance can be calculated by the Norde's method through the relation

$$R_s = \frac{kT(\gamma - \eta)}{qI} \qquad (6)$$

The barrier height and the series resistance values were determined using Eqs. (5) and (6) as 0.61 eV and 6.4 KΩ, respectively.

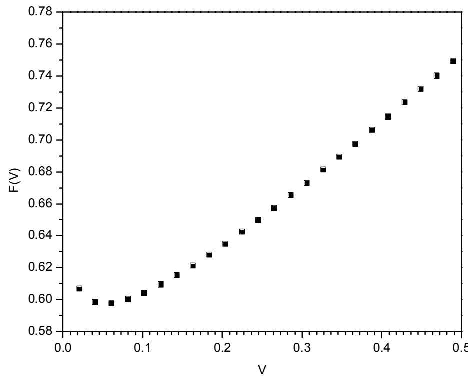

Fig. 3 – *F*(*V*) vs *V* graph of Al/*p*-CuInAlSe$_2$ Schottky diode

S. Cheung's[14] has presented an alternate approach to determine the value of η, φ_{bo} and R_s from I-V measurement . Thus,

$$\frac{d(V)}{d(\ln I)} = R_s I + \left(\frac{\eta kT}{q}\right), \qquad (7)$$

where $\beta = q/kT$. Thus, a plot of $d(V)/d(\ln I)$ vs I will give Rs as the slope and η / β as the y axis intercept. To evaluate φ_{bo}, we can define a function H(I)

$$H(I) = V - \left(\frac{\eta kT}{q}\right)\ln\left(\frac{I}{AA^{**}T^2}\right). \qquad (8)$$

For equation (7) we can deduce

$$H(I) = R_s I + \eta\varphi_{bo}\,. \qquad (9)$$

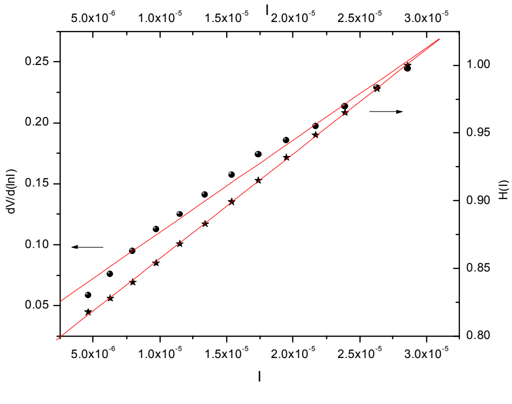

Fig. 4 – Plot of dV/d(lnI) vs I and *H*(I) vs I used to extract the SD parameters

Using the η value determined from equation (7), a plot of H(I) vs I will also give a straight line with y-axis intercept equal to $\eta\varphi_{bo}$. The slope of this plot provides a second determination of R_s which can be used to check the consistency of this approach.

Thus, performing two different plots equations (7) and (9) of the I-V data obtained from one measurement can determine all the three key diode parameters η, φ_{bo} and R_s. We have applied this procedure to characterize Al/*p*-CuInAlSe$_2$ Schottky diodes and various diode parameters so obtained are presented in Table 1.

3.2 Capacitance-Voltage Characteristics

The depletion region of a schottky barrier behaves in some respect like a parallel-plate capacitor. It is important to know what factors determine its capacitance, not only because reverse-biased diodes are used in practice as variable capacitors (varactors), but also because measurements of the capacitance under reverse bias can be used to give information about the barrier parameters [1].

Therefore, for the comparative study, an attempt has been made to access the doping concentration and barrier height from the C^{-2}-V measurement. The C-V relationship as applicable to intimate Metal-Semiconductor Schottky diodes formed on uniformly doped materials can be written as [15]

$$\frac{1}{C^2} = \frac{2(V_o - V_R)}{q\varepsilon_s N_A A^2}, \qquad (10)$$

where ε_s the permittivity of the semiconductor, V_R is the reverse bias voltage, N_A is the acceptor concentration, q is the electronic charge, A is the area of the diode (9×10^{-2} cm^2). The slope of the above plot gives the value of the acceptor concentration (N_a) while the x-intercept of the plot of ($1 / C^2$) versus V_R gives V_o is related to the built-in potential or diffusion potential (V_{bi}) by the equation,

$$V_{bi} = V_o + \frac{KT}{q}, \qquad (11)$$

where T is the absolute temperature in Kelvin.

The zero-bias barrier height (φ_{cv}) from the C-V measurement is defined by

$$\varphi_{cv} = V_0 + \frac{KT}{q} + V_n \quad \text{or} \quad \varphi_{cv} = V_{bi} + V_n, \qquad (12)$$

$$V_n = \left(\frac{kT}{q}\right)\ln\left(\frac{N_v}{N_A}\right), \qquad (13)$$

where V_n is the voltage axis intercept of the plot shown in Fig. 5 and represents the energy difference between the Fermi level and the bottom of the conduction band edge in CuInAlSe$_2$ and

$$N_v = 2\left(\frac{2\pi m_p kT}{h^2}\right)^{3/2}. \qquad (14)$$

N_v is the effective density of states in the conduction band of CuInAlSe$_2$, where m_p is the effective mass of CuInAlSe$_2$ = 0.15 m_0 eV

$$N_A = \left(\frac{2}{q\varepsilon_o\varepsilon_s A^2}\right)\left(\frac{dv}{dc^{-2}}\right) \qquad (15)$$

is the acceptor density of CuInAlSe$_2$, $\varepsilon_s = 8.1$; the dielectric constant of CuInSe$_2$, $\varepsilon_0 = 8.85 \times 10^{-12}$ F m^{-1} ; the permittivity of the free space, $A = 9 \times 10^{-2}$ cm^2; the area of the Schottky diode. Since the value of dielectric constant of CuInAlSe$_2$ is not known, therefore, the va-lue of its close derivative CuInSe$_2$ was used. The value of carrier concentration (N_A) is calculated from the slope of reverse bias C^{-2}-V characteristics is 4.23×10^{19} cm^{-3} in close agreement with that obtained from the electrical analysis of CuInAlSe$_2$ thin films(~ 10^{19} cm^{-3}).

The experimental reverse biased C^{-2} Vs V$_R$ characteristics of the Al/*p*-CuInAlSe$_2$ at room temperature have been shown in Fig. 5. The junction capacitance has been performed at the frequency of 1 MHz. C^{-2}-V characteristics for the Al/*p*-CuInAlSe$_2$ Schottky diodes have also been measured at varying frequencies. The frequency dependent C^{-2}-V characteristics for the Al/*p*-CuInAlSe$_2$ Schottky diode at varying frequency from 50 kHz to 1 MHz are shown in Fig. 6. The slope variation suggests a large density of slow traps or interface states for the prepared schottky diodes [18].

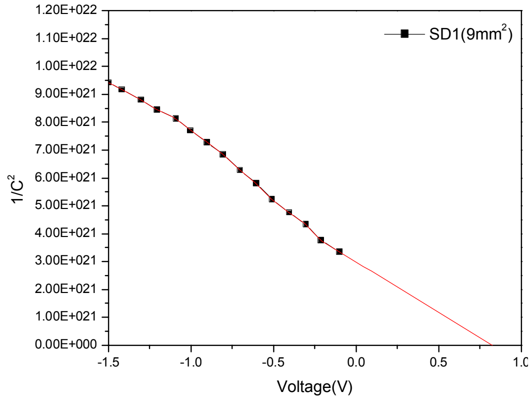

Fig. 5 – Plot of $1 / C^2$ versus V_R of Al/CIAS Schottky Diode at room temperature at 1 MHz frequency

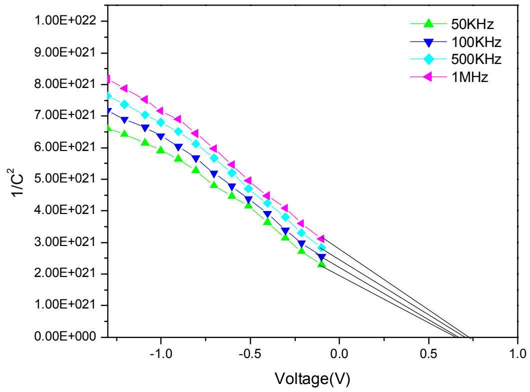

Fig. 6 – Plot of $1 / C^2$versus V_R of Al/CuInAlSe$_2$ Schottky Diode at room temperature at (i) 1 MHz (ii) 500 kHz (iii) 100 kHz (iv) 50 kHz

The barrier height obtained from C^{-2}-V plot has been presented in Table 1. It has been seen that the schottky barrier height deduced from the room temperature I-V analysis at room temperature is less than that obtained from the C-V characteristics. This is may be due to the reason that I-V analysis includes both the image force lowering and dipole lowering effects and is also reduced by the tunneling and leakage currents [18]. However, the capacitance-voltage measurements can be used to directly measure the barrier height. Nevertheless, it has to be noted that the measured capacitance may be considerably influenced by carrier trapping if the lifetime of the trapping levels in the semiconductor is of the same order as the period of the ac signal applied during the capacitance measurement [2, 9, 17, 18, 19].

Table 1 – Comparison of diodes parameters extracted from four different methods.

Parameters	Linear Fitting	Cheung's Method	Norde's Method	C-V Measurement
η	3.79	3.89	---	---
φ_{bo} (eV)	0.50	0.51	0.52	0.60
R_s (KΩ)	---	28	27.5	----

3.3 Energy Band Diagram

The barrier height (φ_{bo}) is related to work function of the metal (φ_m) and the electron affinity (χ) of the semiconductor according to relation

$$q\varphi_{bo} = E_g - q\left(\varphi_m - \chi\right), \tag{16}$$

where E_g is the bandgap of the *p*-type semiconductor ($E_g = 1.24$ eV) and φ_{bo} is the barrier height of Al/*p*-CuInAlSe$_2$ Schottky diode. Assuming work function of the metal (φ_m) as 4.28 V the electron affinity (χ) of CuInAlSe$_2$ in the present case was found to be 3.64 V.

Also, in M-S contact the work function for *p*-type semiconductor can be written as

$$q\varphi_s = q\left(\varphi_m + V_{bi}\right), \tag{17}$$

and is found equal to 4.74 eV. Using the above experimental values of various parameters the equilibrium energy band diagram for the *p*-CuInAlSe$_2$/Al Schottky diode system was constructed and is shown in Fig. 7.

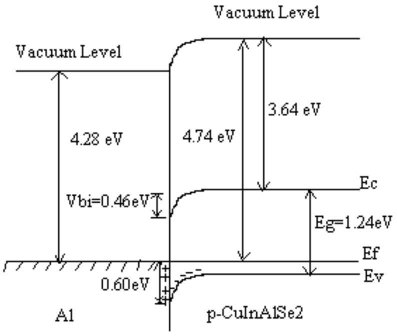

Fig. 7 – Energy band diagram of Al/*p*-CuInAlSe$_2$ Schottky Diode

Since the value of the metal work function is low compared to that of semiconductor (ie. $\varphi_m < \varphi_s$), electrons will move from metal to semiconductor. Each electron flowing into the semiconductor removes a hole from the valance band, leaving neutralized charge of ionized acceptor in the semiconductor and thus, forming a potential barrier at the metal-semiconductor interface region [4]. Since the current in a p-type semiconductor is carried mainly by holes, so the contact of Fig. 7. is a rectifying (or Schottky) contact and the barrier height to the holes flow is 0.60 eV.

4. CONCLUSION

In this study, Al/*p*-CuInAlSe$_2$ Schottky diodes were fabricated over flash evaporated soda lime glass substrates. Various diode parameters like barrier height, ideality factor and series resistance values were calculated by using several methods proposed by different authors. The results obtained from different methods were found in close agreement to each other. However, due to the image force and dipole lowering effects as well as tunneling and leakage currents in I-V characteristics, the barrier height obtained from I-V analysis was found lower to that determined from C-V analysis. Also, the deviation from ideal diode for this structure can be attributed a native interfacial layer at Al-CuInAlSe$_2$ interface. To study the nature of barrier formed at the M-S interface energy band diagram of Al/*p*-CuInAlSe$_2$ Schottky diode was also reconstructed and was found well matched with the predicted current transport model.

ACKNOWLEDGEMENTS

One of the authors (C J Panchal) also wish to thank "University Grants Commission" (UGC), New Delhi, India, for providing the financial assistance through major research project F. no. 40-448/2011 (SR) dated 4th July 2011.

REFERENCES

1. W.N. Shafarman, R. Klenk, B.E. McCandless, *J. Appl. Phys.* **79**, 7324 (1996).
2. T. Markvart, B. Lane, Ch. W. Sussex, *Solar Electricity*. (England: John Wiley & Sons: 2000).
3. S.M. Sze, Ng. Kwok K., *Physics of Semiconductor Devices Hoboken* (New Jersey: John Wiley & Sons, Inc.: 2007).
4. E.H. Rhoderick, R.H. Williams, *Metal-Semiconductor Contacts, 2nd Edition* (Clarendon Press: Oxford: 1978).
5. R.T. Tung, *Mater. Sci. Eng.: R* **35**, 1 (2001).
6. S. Altındal, S. Karadeniz, *Solid State Electron.* **47**, 1847 (2003).
7. P. Chattopadhyay, A.N. Daw. *Solid State Electron.* **29**, 555 (1986).
8. J.P. Sullivan, R.T. Tung, *J. Appl. Phys.* **70**, 7403 (1991).
9. H. Dogan, N. Yilirim, *Semicond. Sci. Tech.* **21**, 822 (2006).
10. R.T. Tung, *J. Vac. Sci. Technol. B* **11**, 1546 (1993).
11. M. Saglam, M. Biber, A. Turut, M.S. Agırtas, M. Cakar, *Int. J. Polym. Mater.* **54**, 805 (2005).
12. H. Norde, *J. Appl. Phys.* **50**, 5052 (1979).
13. S. Karatas, S. Altındal, A. Turut, M. Cakar, *Physica B* **392**, 43 (2007).
14. S.K. Cheung, N.W. Cheung, *Appl. Phys. Lett.* **49**, 85 (1986).
15. A. Turut, M. Saglam, H. Efeoglu, N. Yalcic, M. Yildirim, B. Abay, *Physica B* **205**, 41 (1995).
16. M.S. Tyagi, *Introduction to Semiconductor Materials and Devices* (John Wiley & Sons: New York: 2008).
17. S. Aydogan, M. Saglam, A. Turut, *Polymer* **46**, 6148 (2005).
18. A. Turut, M. Saglam, H. Efeoglu, N. Yalcin, M. Yildirim, B. Abay, *Physica B* **205**, 41 (1995).
19. I. Shih, C.X. Qiu, *J. Appl. Phys.* **63**, 439 (1988).
20. U. Parihar, *J. Nano- Electron. Phys.* **3** No1, 1086 (2011).